Athens Journal of Sciences- Volume 10, Issue 1, March 2023 – Pages 53-64

Snow Height and Snow Water Equivalent Estimation from Snow Cover Fraction Using Sentinel-2 Satellite Images in North Kazakhstan

By Zhanassyl Teleubay[*], Farabi Yermekov[±], Zhanat Toleubekova[°], Bauyrzhan Shmatov[•], Yernar Raiev[♦] & Aigerim Assylkhanova[♣]

Climate change's influence on snowpack can significantly affect natural and anthropogenic processes. Water resources and agri-business, which depend on winter precipitation, are highly affected by variations in a snowbank and melting regimes. This paper demonstrates the comparison results of the snowpack thickness estimation in the LLP "North Kazakhstan AES" adopting distinctive techniques (quadratic, exponential, and linear functions) for assessing Fractional Snow Cover (SCF) and demonstrating Snow Water Equivalent (SWE) on the one hand, and in-situ perspective on the other. Between the 26–29 of February 2020, a field measurement was managed on the territory of 25,000 hectares. Accordingly, the thickness of the snowpack was surveyed at 560 points, and its density was measured at 70 points. Applying existing methodologies of SCF computation, it became apparent that the quadratic equation provides more reliable results at RMSE of 0.01 m, followed by linear -0.12 m and exponential -0.13 m methods. This work showed a strong correlation between snow height and SCF, namely the quadratic function in Northern Kazakhstan. Thus, we strongly suggest using Sentinel-2 MSI and the quadratic SCF estimation function for snow cover estimation, further spring flood forecasting, and other hydrological studies.

Keywords: *snow height, snow cover fraction, normalized-difference snow index, snow water equivalent, Sentinel-2 MSI, North Kazakhstan*

Introduction

Due to the high natural spatio-temporal variability of the snow cover and its quick directional changes caused by the changing climate, the development of techniques for acquiring accurate information on the snow cover with high spatial and temporal resolution across broad areas is crucial (Armstrong and Brun 2008). Snow cover impacts nearly all processes of interaction of the atmosphere with the underlying surface of temperate and high latitudes in the cold season because of thermophysical solid properties, the significant fluctuation of parameters, and the

[*]Head, Big Data Analysis Laboratory, S.Seifullin Kazakh Agrotechnical University, Kazakhstan.
[±]Head, CTC in the Field of Digitalization of Agro-Industrial Complex, S.Seifullin Kazakh Agrotechnical University, Kazakhstan.
[°]Dean, Faculty of Land Management, Architecture, and Design, S.Seifullin Kazakh Agrotechnical University, Kazakhstan.
[•]Big Data Analysis Laboratory Specialist, S.Seifullin Kazakh Agrotechnical University, Kazakhstan.
[♦]Big Data Analysis Laboratory Specialist, S.Seifullin Kazakh Agrotechnical University, Kazakhstan.
[♣]PhD Candidate, University of Szeged, Hungary.

https://doi.org/10.30958/ajs.10-1-4 doi=10.30958/ajs.10-1-4

duration of occurrence across broad land regions (Varvus 2007). An important influence on natural and artificial systems may result from the effect of global warming on snow cover (early snowmelt, shorter period with stable snow cover). Since the snow cover in the mountainous and lowland areas of the temperate climate zone is more subject to temperature fluctuations, snowmelt is most likely to increase in these areas in the near future (Popova et al. 2015). The water resources (changes in the intensity of spring floods, greater capacity for evaporation) and the agriculture sectors that depend on them are impacted by variations in the regime of snow accumulation and snow melting (Barnett et al. 2005).

The soil and climatic conditions of the region of Northern Kazakhstan are ideal for the growth of cereals, oilseeds, legumes, and forage crops, and, in particular, for the production of food spring soft wheat with high content gluten, which is in high demand on global markets due to its property of enhancing the baking properties of flour. Peas, lentils, rapeseed, sunflowers, flax, spring wheat, millet, and oats occupy a significant part of the land (Shur 2014). Because of its position, the North Kazakhstan region's agricultural fields receive natural irrigation from rainfall and moisture stored in the soil from snowmelt. To get the best harvest of farm fields, particularly winter crops, it is necessary to know how much snow was melted in a particular location and whether there is enough moisture in the soil.

It is known that the thermal conductivity and density of the snow cover increase with increasing snow depth. Loose, recently fallen snow has the lowest heat conductivity and has the most significant insulating impact on winter crops. On the other hand, compacted snow offers less protection from freezing to winter crops. Since a decrease in soil temperature at this depth up to a certain point damages the tillering node and frequently results in plant death, the question of how snow cover affects soil temperature at a depth of winter crops' tillering nodes (3-5 cm) is of particular interest to the agricultural industry. The soil temperature at the level of tillering node, therefore, turns out to be 1-3°C higher than the air temperature in the presence of a snow cover between 1 and 5 cm thick (Ventskevich 1952). The average thickness of the snow cover in Kazakhstan's northern areas is between 40 and 70 cm, according to the "Map of the Depth of Snow Cover" (Richter 1948).

To determine the safety of winter crops in crucial fields of the North Kazakhstan region in the third decade of February 2020, this study will estimate the snow height (SH) and snow water equivalent (SWE) from SCF maps derived using NDSI and different regression equations. The depth of water that may occur if the snow were to melt entirely is known as the snow water equivalent (SWE). It can describe a restricted snow pattern over a matching specified surface area or snow cover over a specific region. The snow water equivalent is calculated by multiplying the vertically integrated density in kilograms per cubic meter by the snow depth in meters (Goodison et al. 1981).

Study Area

The research was conducted in the territory of the agricultural enterprise "North Kazakhstan AES," located in the Aqqayin district in the North Kazakhstan region (54° 17′ N, 69° 52′ E). On the 72 thousand hectares shown territory, of which the arable land and agricultural fields cover almost 25 thousand ha, the study area's characteristics include relatively level relief and the existence of several lakes (see Figure 1).

Figure 1. *DEM of the LLP "North Kazakhstan AES"*

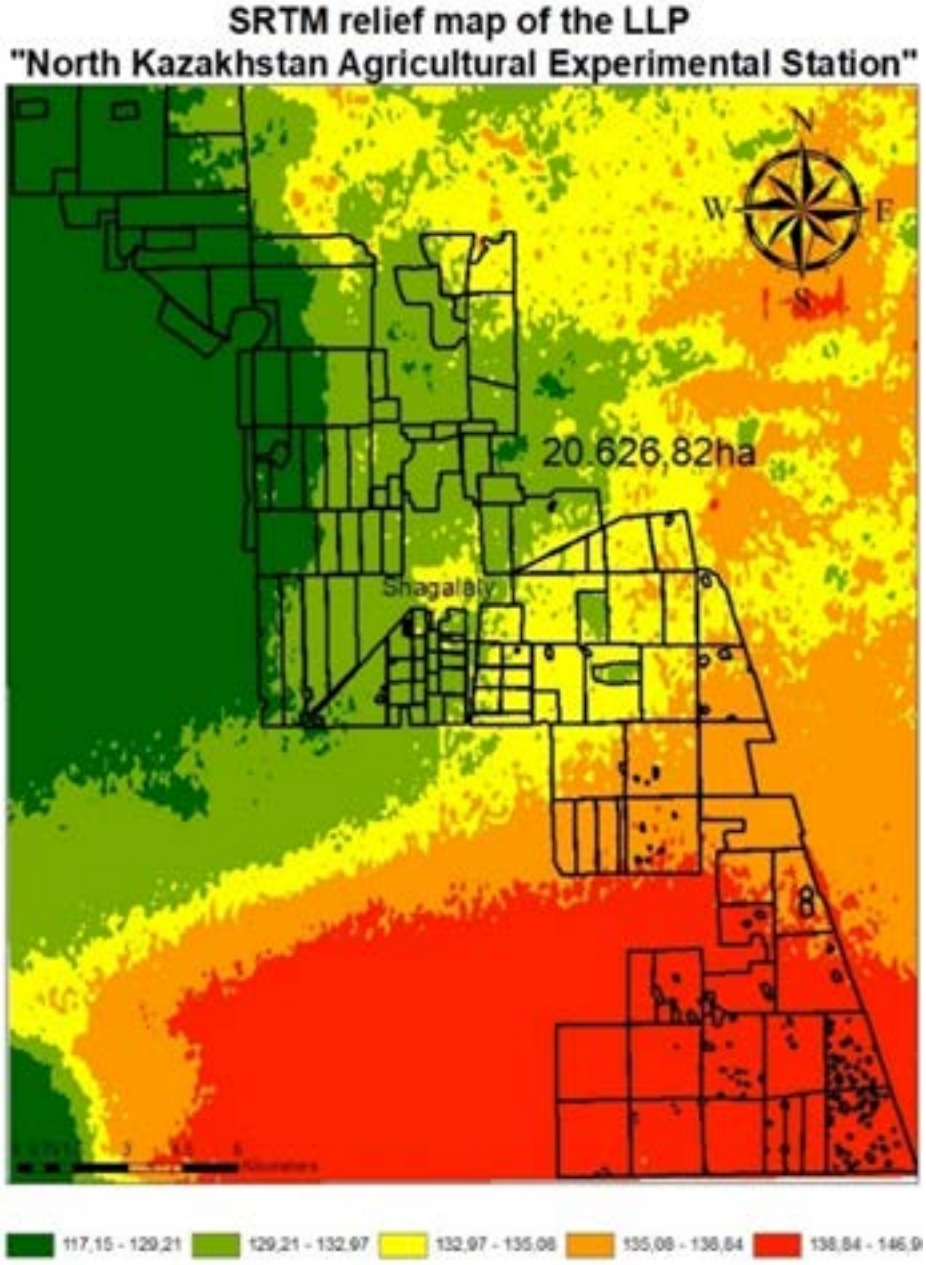

Source: Compiled by the authors.

According to the Gismeteo data, the southwest wind was predominant throughout the field snow survey, reaching a maximum speed of 13 m/s and an average value of 6.4 m/s (Gismeteo 2020). A preponderance of south-southwestern points was another characteristic of the wind direction for the cold spell of 2019–2020. The direction of the wind is of great importance as it affects the thickness of the snow cover; snow from the tops of the hills is blown away by the wind and accumulates in depressions and ravines at the base of the slopes.

Materials and Methods

Snow height, density, Snow Cover Fraction (SCF), and Snow Water Equivalent (SWE) may be measured both in-situ and via remotely sensed data. The snow-water equivalent is a crucial cryospheric research parameter since snow, water, and ice are essential to agriculture and the climate system.

Ground-Truth Field Survey

From February 26 to February 29, 2020, a field snow survey was conducted at prominent locations. Over the area of LLP "North Kazakhstan AES," the snow cover was assessed at 560 points (snow height and density). A metal ruler with a 1-mm scale was used to measure the thickness of the snow, and the weight snow gauge VS-43 was used to determine the snow's density. We employed a snowmobile that belonged to the S. Seifullin Kazakh Agrotechnical University's scientific and educational center of GIS technologies for rapid and easy mobility across the research region (see Figure 2). The mass (m) of measured snow and the height (SH) of measured snow were used to compute the actual density (ρ) of snow:

$$\rho = \frac{m}{10 \times SH} \quad (1)$$

where ρ is in kg/m^3, SH in m, and m in kg.

Figure 2. *Measurement of Snow Height and Density Using a Weight Snow Gauge (VS-43)*

Source: Compiled by the authors.

However, the literature has several approaches for calculating snow density with minimal input parameters. We especially want to highlight Sturm et al.'s (2010) study, which offers a variety of highly straightforward solutions for snow density that are accessible through a single equation:

$$\rho = \rho_0 + (\rho_{\max} - \rho_0) \times (1 - \exp\left(-k_1 \times HS - k_2 \times \frac{DOY}{100}\right)), \quad (2)$$

where variables ρ_0, ρ_{max}, k_1 and k_2 are accessible in Table 1, and DOY is a simple day of the year which starts with -92 on October 1 to -1 on December 31 and from 1 on January 1 till 181 on June 30.

Table 1. *The Set of Variables of Snow Classes for the Equation 2*

Snow class	**ρ_0**	**ρ_{max}**	**k_1**	**k_2**
Alpine	223.7	597.5	0.12	0.38
Maritime	257.8	597.9	0.10	0.38
Steppe	233.2	594.0	0.16	0.31
Tundra	242.5	363.0	0.29	0.49
Taiga	217.0	217.0	0	0

Source: Sturm et al. 2010.

For the Snow Water Equivalent (SWE) calculation, a simple formula was utilized:

$$SWE = \rho \times SH. \quad (3)$$

where SWE is in kg/m^2, ρ in kg/m^3 and SH in m.

Remote Sensing Data

We took the multispectral satellite images of Sentinel-2 MSI with the product ID:
S2B_MSIL1C_20200308T062709_N0209_R077_T42UWF_20200308T092518
and
S2B_MSIL1C_20200308T062709_N0209_R077_T42UWE_20200308T092518
and performed the whole data processing flow to compute the snow height (SH) and snow water equivalent (SWE) from Normalized-Difference Snow Index (NDSI) (see Figure 3).

Figure 3. *Flow Chart for Data Processing Methods*

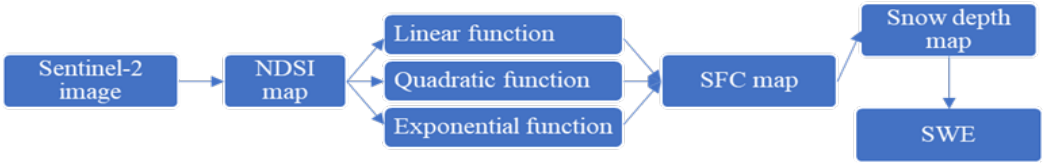

Source: Compiled by the authors.

The NDSI is based on the variation in how well snow absorbs light in the visible and infrared spectrums. Thus, the method is only used during the day, evening, or night. Pixels coated in ice will not be seen (Kim et al. 2017). The difference between the reflectance of light from Sentinel-2 with wavelengths of 560 nm (Band 3) and 1610 nm (Band 11) is used to construct the NDSI index.

$$NDSI = \frac{B_3 - B_{11}}{B_3 + B_{11}}. \quad (4)$$

where B3 is the Green band, and B11 is the SWIR band of Sentinel-2 MSI. Once the Normalized-Difference Snow Index is calculated, we can define the area covered by snow as having pixel values higher than 0.4.

Calculating the Snow Cover Fraction (SCF) within each picture pixel is the most crucial step in modeling the snow height using RS data. It ranges from 0 to 1 and shows the percentage of the snow-covered pixel (0 percent - 100 percent). Three NDSI SCF estimate formulae are currently available in the literature:

1. linear function (Salomonson et al. 2004)

$$SCF = a + b \times NDSI. \quad (5)$$

where a and b are constants equal to -0.69 and 1.91, respectively.

2. quadratic function (Barton et al. 2000)

$$SCF = a + b \times NDSI + c \times NDSI^2. \quad (6)$$

where a. b, and c are optimized constants equal to 0.18. 0.37 and 0.25, respectively.

3. exponential function (Lin et al. 2012)

$$SCF = a + b \times e^{c*NDSI}. \quad (7)$$

where a. b and c are equal to -0.41. 0.571 and 1.068, respectively.

Romanov and Tarpley (2004) discovered a high correlation between SCF and SH during the calculation of snow height (SH), as the snow height rose with increasing Snow Cover Fraction. They have suggested the following equation based on this observation:

$$HS = e^{a*SCF} - 1, \quad (8)$$

where a is equal to 0.33.

The SH was estimated using the formulas (7) and (8); then, they were validated by ground-truth snow surveying results. Furthermore, we calculated the SWE using equation (3).

Results

Using the linear, quadratic, and exponential equations as stated before, Figure 4 demonstrates the Normalized-Difference Snow Index (NDSI) and Snow Cover Fraction (SCF) maps of the study area. Due to the weather conditions in Northern Kazakhstan and the DOY when the image was taken, 99 percent of the research area was covered in snow. Therefore, there was no need to mask the NDSI map. The results from the exponential and linear equations are almost identical. However, the figures for the snow percentage from the quadratic equation are relatively low. Nevertheless, the three SCF maps' patterns do not differ much.

Figure 4. *Normalized-Difference Snow Index (NDSI) and Snow Cover Fraction (SCF) Maps (a) Linear, (b) Quadratic, (c) Exponential Equations*

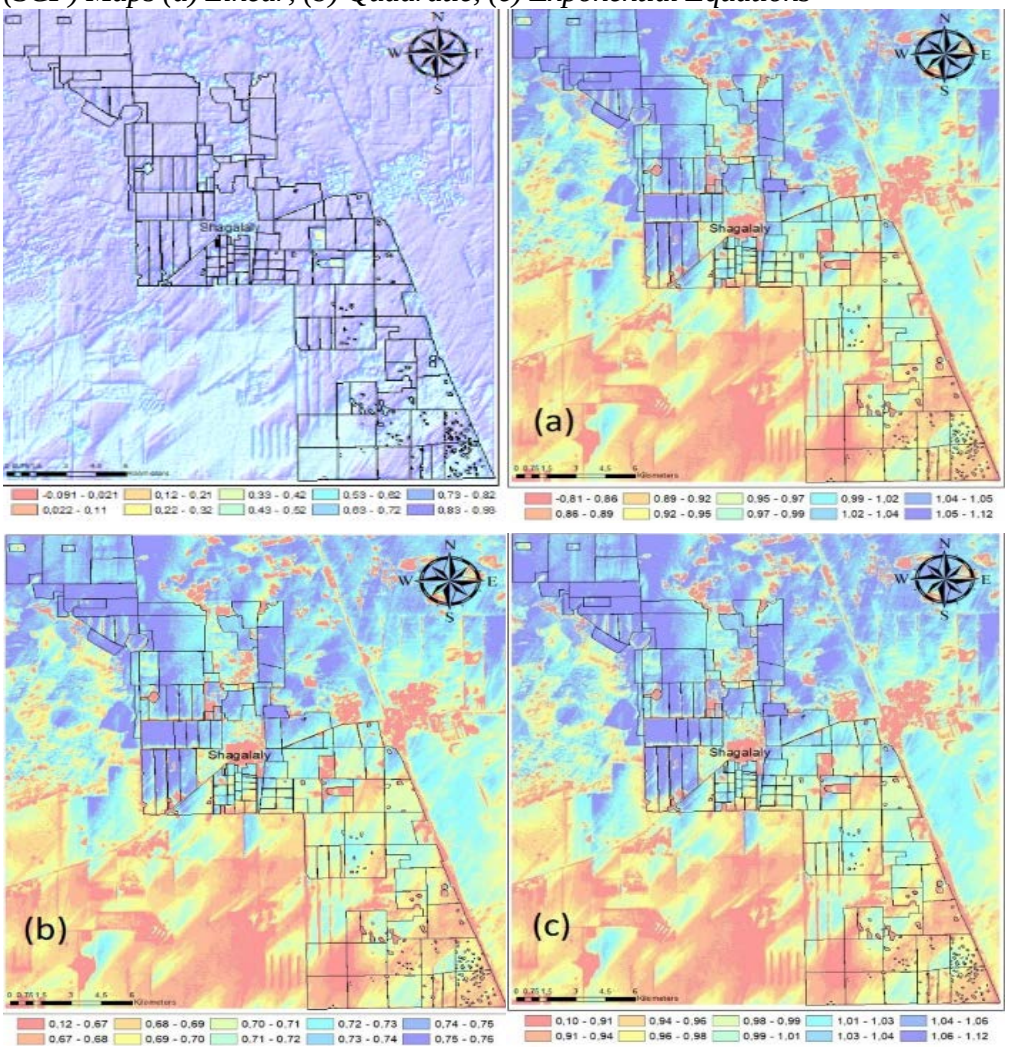

Source: Compiled by the authors.

The equation (8) for each SCF calculation method, including the linear, quadratic, and exponential SH equations, was used to create the snow height maps (see Figure 5). The variances are more pronounced since the same algorithm was used to estimate the snow depth for each image. The maximum snow height for the SH maps based on the exponential and linear formulae was around 0.45 m, whereas the maximum snow height for the quadratic equation was only about 0.28 m.

Figure 5. *Snow Height (SH) Maps Generated Using (a) Linear, (b) Quadratic, and (c) Exponential Equations of SCF*

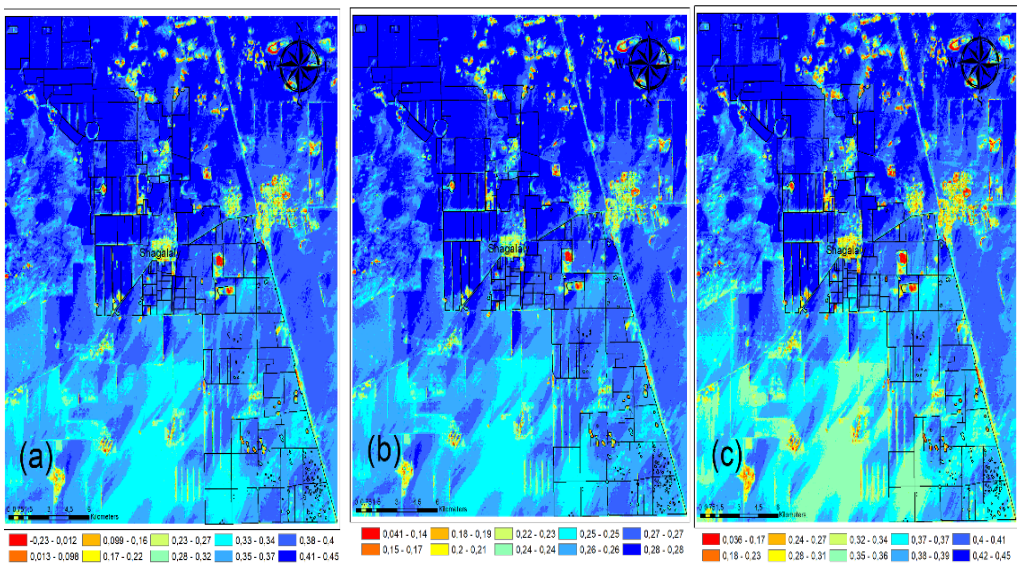

Source: Compiled by the authors.

With a root-mean-square error (RMSE) of 0.12 m for linear equations, 0.01 m for quadratic equations, and 0.13 m for exponential equations, we further showed the correlation between the ground-truth snow height and modeled snow height maps (see Figure 6). Due to the SCF's negative representation, the snow height frequently has a negative value in the linear equation. Since the variables were overestimated at the SCF level calculation, the snow height value is often low in the quadratic function. In contrast to the other two situations, the data in the exponential approach is typically significantly more confusing.

Figure 6. *Validation of Simulated SH Maps with (a) Linear, (b) Quadratic, and (c) Componential Equations by Comparing with the Ground-Truth SH Values*

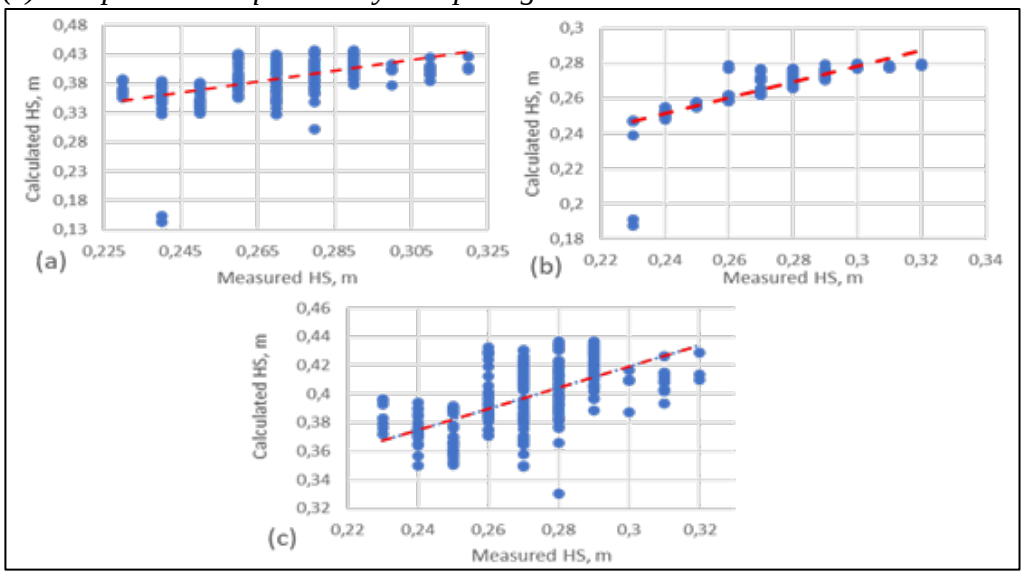

Source: Compiled by the authors.

Overall, based on the statistical data, we chose to use the SH map produced using the quadratic function of SCF calculation to determine the final Snow Water Equivalent (SWE). Equation (3) was used to calculate the result, and the quadratic equation's snow height (SH) was multiplied by the average observed snow density (ρ_{avg}=216 kg/m^3) (see Figure 7). It is evident from the map that the southwest wind impacted the amount of snow that accumulated behind the objects on the opposite northeast side because of the swirl and in the low-elevation places. Additionally, the southern agricultural fields had at least 1 cm less snow cover, while the low-lying northern area of the LLP "North Kazakhstan AES" preserved substantially more snow.

Figure 7. *Modeled Snow Water Equivalent (SWE) in the Study Area in kg/m^2*

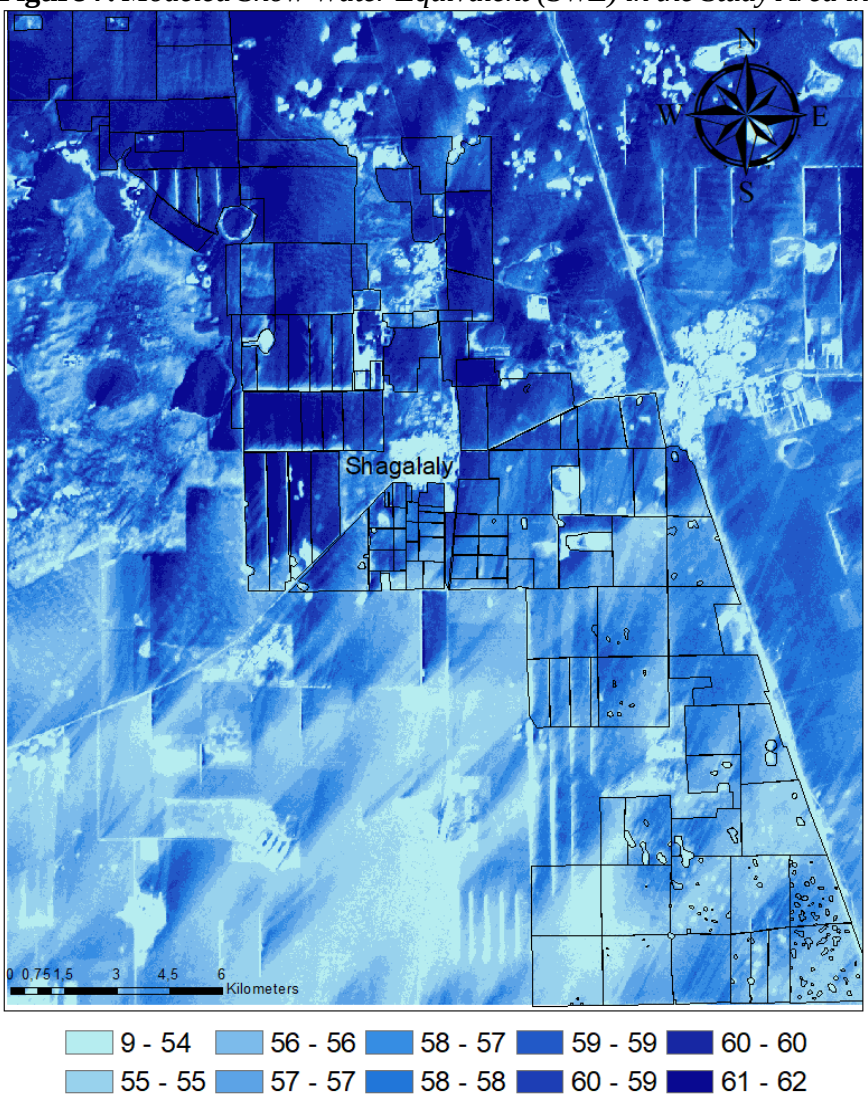

Source: Compiled by the authors.

This study applied the recommended SCF calculation technique to a straightforward Sentinel-2 multispectral image using NDSI, and three different snow height (SH) maps were produced from the estimated SCF. Several factors

affect SCF and NDSI, although NDSI and SCF have a reasonable correlation. Additionally, each method's formula is specifically designed for study fields other than the region of northern Kazakhstan. Moreover, it should be noted that in the metropolitan, built areas, the snow disappears because of the snow removal even if there is a measured in-situ snow height (SH); thus, there can be an error.

Conclusion

We applied three different regression methods of calculating the Snow Cover Fraction to data from the LLP "North Kazakhstan AES" to simulate snow height using remotely sensed images and NDSI. The results were compared as a first step toward developing an optimization to measure the snow depth in the study area. The actual ground-truth snow height was used to verify the modeled snow height. The quadratic formula (0.01 m) produced the best results, followed by the linear (0.12 m) and exponential (0.13 m) equations in terms of RMSE. The lowest snow level was predominantly found inside built-up areas, and settlements on the SH map were produced using a quadratic equation and accounted for 4-5 cm. The study area's northernmost region, where the elevation was lowest according to the SRTM DEM, had the thickest snow cover, which was 28 cm. The average snow depth in agricultural fields was 20 cm, which is more than safe for winter crops because even 3-5 cm of snow may raise the temperature of seeds by 1-3°C in comparison to the air, and this quantity of snow, when melted, can add enough moisture to the soil to make it very fruitful. According to the produced SWE map, the lowest water level recorded was 8 mm, the average was 45 mm, and the maximum level was more than 60 mm. At least for the Northern Kazakhstan region, we can confidently assert that the quadratic equation of the SCF calculation suits the best, and it offers a fantastic potential to produce trustworthy SWE maps.

References

Armstrong RL, Brun E (2008) *Snow and climate*. Cambridge University Press.

Barnett TP, Adam JC, Lettenmaier DP (2005) Potential impacts of a warming climate on water availability in snow-dominated regions. *Nature* 438(Nov): 303–309.

Barton JS, Hall DK, Riggs GA (2000) Remote sensing of fractional snow cover using Moderate Resolution Imaging Spectroradiometer (MODIS) data. In *Proceedings of the 57th Eastern Snow Conference*, 171–183. Syracuse, New York, USA, May 17-19.

Gismeteo (2020) *Weather diary for Chagalaly for February 2020*. MapMakers Group Ltd., Gismeteo.

Goodison BE, Ferguson HL, McKay GA (1981) Measurement and data analysis. In *Handbook of Snow*, 191–274. Reprint. Caldwell, NJ, USA: The Blackburn Press.

Kim D, Jung H-S, Kim J-C (2017) Comparison of snow cover fraction functions to estimate snow depth of South Korea from MODIS imagery. *Korean Journal of Remote Sensing* 33(4): 401–410.

Lin J, Feng X, Xiao P, Li H, Wang J, Li Y (2012) Comparison of snow indexes in estimating snow cover fraction in a mountainous area in northwestern China. *IEEE Geoscience and Remote Sensing Letters* 9(4): 725–729.

Popova VV, Morozova PA, Titkova TB, Semenov VA, Cherenkova EA, Shiryaeva AV, et al. (2015) Regional features of present winter snow accumulation variability in the North Eurasia from data of observations, reanalysis and satellites. *Ice and Snow* 55(4): 73–86.

Richter GD (1948) *The role of snow cover in the physical and geographical process*. Publishing House of the Academy of Sciences of the USSR.

Romanov P, Tarpley D (2004) Estimation of snow depth over open prairie environments using GOES imager observations. *Hydrological Processes* 18(6): 1073–1087.

Salomonson VV, Appel I (2004) Estimating fractional snow cover from MODIS using the normalized difference snow index. *Remote Sensing of Environment* 89(3): 351–360.

Shur AV (2014) Natural and economic factors of formation of agrarian specialization in the Republic of Kazakhstan. *Pskov Regionalological Journal* 20: 46–54.

Sturm M, Taras B, Liston G, Derksen C, Jonas T, Lea J (2010) Estimating regional and global snow water resources using depth data and climate classes of snow. *Journal of Hydrometeorology* 11(6): 1380–1394.

Vavrus S (2007) The role of terrestrial snow cover in the climate system. *Climate Dynamics* 29(Feb): 73–88.

Ventskevich GZ (1952) *Agricultural meteorology*. Leningrad: Hydrometeorological Publishing House.